Available online at www.sciencedirect.com
ScienceDirect
Journal of Solid State Chemistry 181 (2008) 783–788
JOURNAL OF SOLID STATE CHEMISTRY
www.elsevier.com/locate/jssc

Solid-state synthesis in the system $Na_{0.8}Nb_yW_{1-y}O_3$ with $0 \leqslant y \leqslant 0.4$: A new phase, $Na_{0.5}NbO_{2.75}$, with perovskite-type structure

Tapas Debnath[a,*], Claus H. Rüscher[a], Thorsten M. Gesing[a], Jürgen Koepke[a], Altaf Hussain[b]

[a]*Institute of Mineralogy, Leibniz Universität Hannover, D-30167 Hannover, Germany*
[b]*Department of Chemistry, University of Dhaka, Bangladesh*

Received 23 November 2007; received in revised form 11 January 2008; accepted 12 January 2008
Available online 26 January 2008

Abstract

Series of compounds in the system $Na_xNb_yW_{1-y}O_3$ were prepared according to the appropriate molar ratio of Na_2WO_4, WO_3, WO_2 and Nb_2O_5 with $x = 0.80$ and $0.0 \leqslant y \leqslant 0.4$ at 600 °C in evacuated silica glass tubes. These compounds were investigated by X-ray powder diffraction, optical microscopy, microprobe analysis, Raman and optical microspectroscopy. A y-dependent separation into three distinct coloured crystallites with cubic perovskite-type structures is observed: (i) red-orange crystallites with composition Na_xWO_3 with slightly decreasing x (i.e. 0.8–0.72) with increasing nominal y, (ii) bluish solid solution of composition $Na_xNb_yW_{1-y}O_3$ and (iii) white crystallites of a new phase having defect perovskite-type structure with composition $Na_{0.5}NbO_{2.75}$.

Keywords: Tungsten bronze; Perovskite

1. Introduction

Investigations of perovskite tungsten bronzes (PTB) have in many respects a long-standing history (see review articles, [1–4]) and have attracted renewed interest because of their interesting electric, magnetic and optical properties with respect to their variation in composition [5–10]. Sodium tungsten bronzes, Na_xWO_3, with $x \geqslant 0.4$ may be regarded as a prototype system of cubic PTB_c of variable stoichiometry with tungsten in +5 and +6 oxidation states. The formula of Na_xWO_3 can be formally written as $Na_x(W_x^{5+}W_{1-x}^{6+})O_3$ where sodium acts as an electron donor. Sufficiently doped sodium in Na_xWO_3 ($x \geqslant 0.4$) shows metallic property and cubic symmetry. It has been reported [11–13] that pentavalent tungsten ions (effective Shannon radius $r = 76$ pm, coordination number, CN = 6) can be replaced by other pentavalent ions of suitable sizes such as Nb^{5+} ($r = 78$ pm, CN = 6), and Ta^{5+} ($r = 78$ pm, CN = 6), which results in a decrease of the electrical conductivity due to the d° character of Nb^{5+} and Ta^{5+}. Weller et al. [11] obtained a substitution up to about 10% of niobium and tantalum in sodium tungsten bronzes by electrolytic reduction method. Miyamoto et al. [12] synthesized a series of niobium containing solid solution, $NaNb_{1-y}W_yO_3$, at high temperature (1550 °C) and high pressure (6 GPa) and could observe the formation of cubic phases of compositions $y \approx 0.16$ and for $0.52 \leqslant y \leqslant 1$. Dubson et al. [13] prepared tantalum-substituted sodium tungsten bronzes, $Na_xTa_yW_{1-y}O_3$, by electrolytic reduction method.

Our aim was to investigate the effect of substitution of W by Nb in non-stoichiometric PTB by conventional solid-state synthesis method at moderate temperatures as is usually used for the preparation of Na_xWO_3 compositions. It is seen that this is possible but only at low Nb content. For high Nb content, it appears in a mixed phase system with a new type of cubic perovskite bronze of composition $Na_{0.5\pm0.05}NbO_{2.75}$ and the ordinary Na_xWO_3 phase.

2. Experimental

Starting materials were reagent grade (Alfa Aesar) chemicals, $Na_2WO_4 \cdot 2H_2O$ (99.9%), WO_3 (99.998%),

*Corresponding author. Fax: +49 511 762 2995.
E-mail address: tapas.debnath@mineralogie.uni-hannover.de (T. Debnath).

0022-4596/$ - see front matter © 2008 Elsevier Inc. All rights reserved.
doi:10.1016/j.jssc.2008.01.027

WO_2 (99.9%) and Nb_2O_5 (99.9985%). Both WO_3 and Nb_2O_5 were preheated 24 h in air at 700 °C before use. Anhydrous Na_2WO_4 was prepared by heating $Na_2WO_4 \cdot 2H_2O$ in air at 150 °C for 24 h. The purity of all reactants was checked before use by taking X-ray powder *patterns*.

Nominal compositions of $Na_xNb_yW_{1-y}O_3$ where $x = 0.8$ and $0.0 \leqslant y \leqslant 0.4$ were prepared according to the following equation:

$$x/2\ Na_2WO_4 + (1 - x - y/2)WO_3 + (x - y)/2\ WO_2 + y/2\ Nb_2O_5 = Na_xNb_yW_{1-y}O_3. \quad (1)$$

A series of Na_xWO_3 with $0.4 \leqslant x \leqslant 0.8$ samples have also been prepared according to the following equation:

$$x/2\ Na_2WO_4 + (1 - x)WO_3 + x/2\ WO_2 = Na_xWO_3. \quad (2)$$

The appropriate molar ratio of reactants were mixed intimately in an agate mortar and transferred into clean, dry silica tubes (6 mm inner diameter and about 100 mm in length), evacuated (0.13 Pa) at room temperature for 2 h and then sealed. Series of sample prepared in this way were heated in a Muffle furnace at a temperature of 600 °C for 7 days. The ampoules were quenched to room temperature.

The products were characterized by X-ray powder patterns recorded in a Stoe Stadi P diffractometer (transmission geometry, Cu$K\alpha_1$ radiation by a focusing Ge (111) monocromator, linear PSD). Structure refinements were performed using the Rietveld software Diffrac Plus TOPAS (Bruker AXS, Karlsruhe, Germany). For the calculation of the reflex profiles, fundamental parameters were used on the basis of instrumental parameters calculated from a silicon standard measurement. As an additional general parameter, the zero point of the centre was varied and a polarization parameter was fixed. For the structure calculation, a cubic perovskite structure-type model ($Pm\bar{3}m$) was used. The cell parameter of single-phase samples was investigated by taking X-ray powder photographs in a Guinier–Hägg focusing camera (Cu$K\alpha_1$) using Si as internal standard. The patterns were evaluated by scanning films with the aid of a film scanner [14]. The powder patterns of the samples were indexed and the lattice parameters refined with the program PIRUM [15]. To calibrate lattice parameter, series of Na_xWO_3 with $0.4 \leqslant x \leqslant 0.8$ were prepared by the same method as described above. It was observed that the cell parameter data of Na_xWO_3 have excellent agreement with the lattice parameter values reported by Brown and Banks [16] according to Eq. (3):

$$a_c(x) \text{ in pm} = 378.45 + 8.21x. \quad (3)$$

For optical microscopy, polycrystalline samples were glued to plane sample holder (ordinary glass) and mechanically abraded and finally polished (0.2 μm diamond paste) to show optically high-quality surfaces. For microprobe analysis (Electron beam-Microprobe CAMECA SX-100), the polished samples were coated with a carbon layer. Optical micrographs were taken in reflection mode using a Leica microscope with an attached CCD camera (Sony). The optical reflectivity was measured using a FTIR spectrometer (Bruker IFS88) with an attached microscope. Raman measurements were performed on polished samples using a confocal Raman microscope (CRM 200, frequency doubled Nd:YAG laser with maximal power of 20 mW). All spectra were obtained in backscattering geometry using a microscope device that allows the incident light to be focused on the sample as a spot of about 2 μm in diameter.

3. Results and discussion

Optical micrographs (reflection mode) of samples with a nominal composition $0.25 \leqslant y \leqslant 0.4$ show a mixture of crystallites with three different colors: red-orange, bluish and white. A representative example is shown for a sample of nominal composition $y = 0.4$ in Fig. 1. Micrographs of samples with nominal composition $0.0 \leqslant y \leqslant 0.07$ show only red-orange crystals. For $y = 0.1$, bluish *particles* appear which increase in contribution with increasing nominal y. The X-ray diffraction pattern for $0.0 \leqslant y \leqslant 0.07$ samples could uniquely be refined as single cubic PTB_c phase (Fig. 2a). With a further increase in nominal niobium content ($y \geqslant 0.1$), there is a splitting of all diffraction peaks corresponding to two cubic phases of well-separated lattice parameters as shown for the $y = 0.2$ sample (Fig. 2b). For the samples with nominal niobium content $y \geqslant 0.25$, a third characteristic diffraction peak (Fig. 2c) appears. This peak could well be described in a three-phase Rietveld refinements as a third cubic phase as shown in Fig. 2c for the

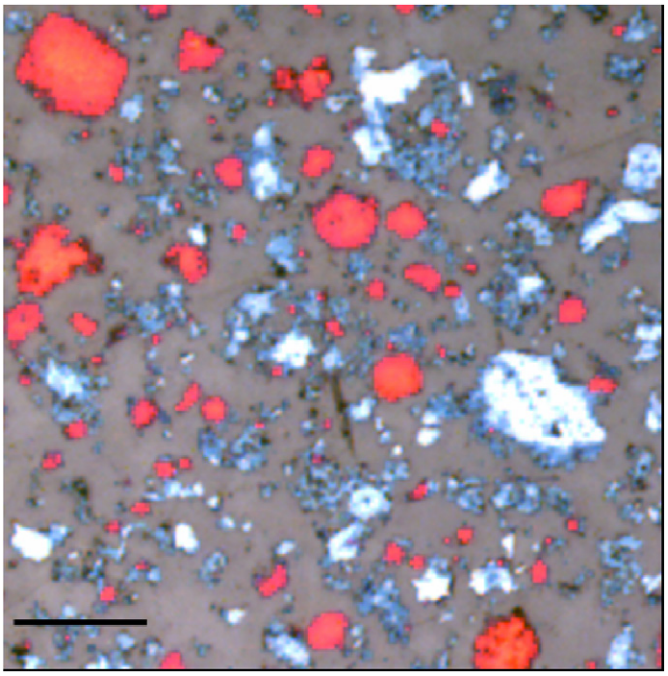

Fig. 1. Optical micrograph of a polished sample of nominal composition $Na_{0.8}Nb_{0.4}W_{0.6}O_3$ showing a mixture of three different coloured crystals: red, light blue and white. The scale bar is 30 μm.

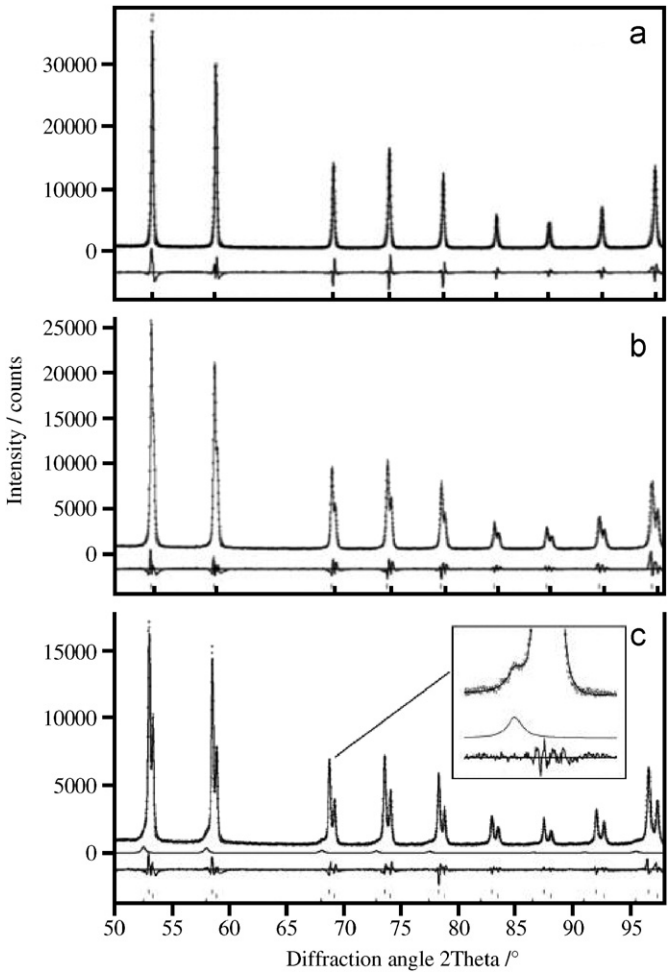

Fig. 2. Observed (solid line) and refined (dotted) XRD pattern for samples of nominal composition $Na_{0.8}Nb_yW_{1-y}O_3$: (a) $y = 0.07$, (b) $y = 0.20$ and (c) $y = 0.40$. The respective difference curve and indexed peak positions (bars) are also shown. For $y = 0.40$ (c), the additional refined pattern of the third phase is shown separately. Inset shows an enlarge scale for 2 2 0 peaks.

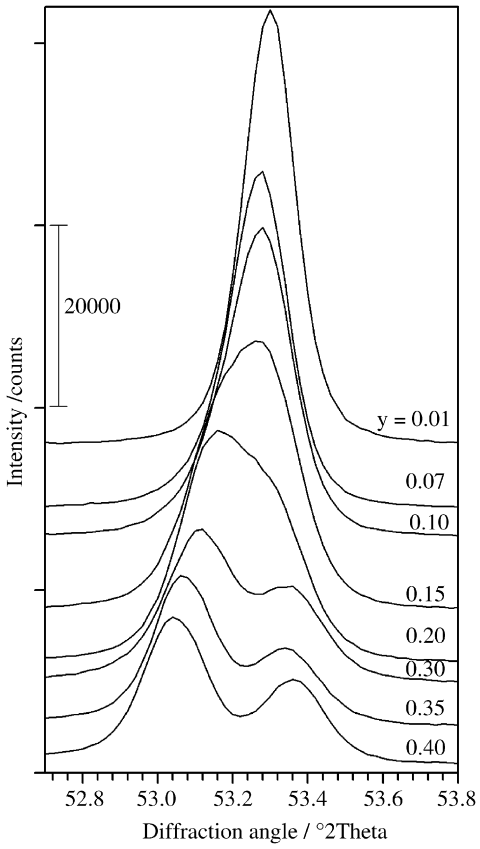

Fig. 3. An enlarged view of 2 1 0 X-ray diffraction peak of samples $Na_{0.8}Nb_yW_{1-y}O_3$ showing a systematic development of second phase for $y \geqslant 0.1$. The peaks are shifted vertically for the sake of clarity.

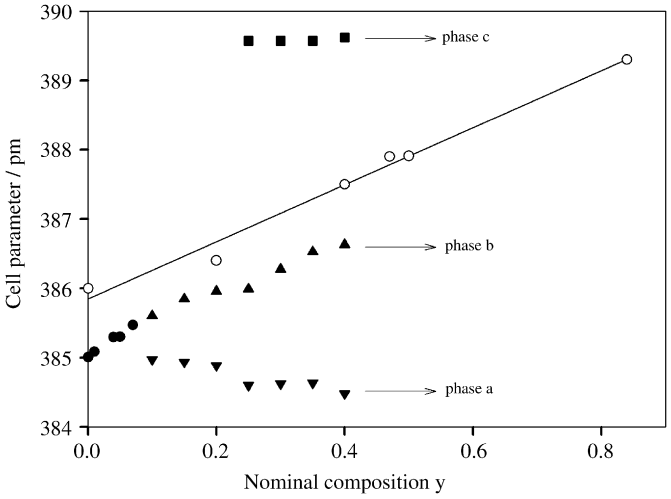

Fig. 4. The refined cell parameter of products from nominal composition $Na_{0.8}Nb_yW_{1-y}O_3$ (closed symbols) compared with that of the reported (open circles) for cubic and pseudo-cubic $NaNb_yW_{1-y}O_3$ system [12]. Single phase (closed circles), two phases (closed triangle top down, "phase *a*") and three phases (closed triangle top up, "phase *b*" and closed square "phase *c*") refinement were done for samples with nominal composition $y = 0.0$–0.07, 0.10–0.20 and 0.25–0.40, respectively.

$y = 0.4$ sample. Because of the strong peak overlapping in the low 2θ range caused by instrumental and average crystal size peak broadening, refinements were carried out using data above 50° 2θ. The well separation of diffraction peaks above 50° 2θ increase the quality of Rietveld refinement. The single-phase samples ($0 \leqslant y \leqslant 0.07$) were refined using 20–$100^\circ$ 2θ. For better comparison, the effect of phase separation into the two leading perovskite-type phases is shown more clearly in Fig. 3 for the 2 1 0 diffraction peak. There is a gradual decrease in peak height together with growing of a low angle shoulder with increasing y which becomes significant in the refinement at $y = 0.10$. The refined lattice parameters of the phases and their relative contributions are plotted in Figs. 4 and 5, respectively. There is a systematic decrease in lattice parameter value for "phase *a*" and an increase for "phase *b*" related on increasing nominal y whereas for "phase *c*" the lattice parameter values remain constant. The relative contributions in the two-phase range show approximately complementary behaviour for *a* (decrease) and *b* (increase) up to $y = 0.25$. For $y \geqslant 0.25$, the contributions of "phase *b*" saturate or even tend to decrease whereas the contribution

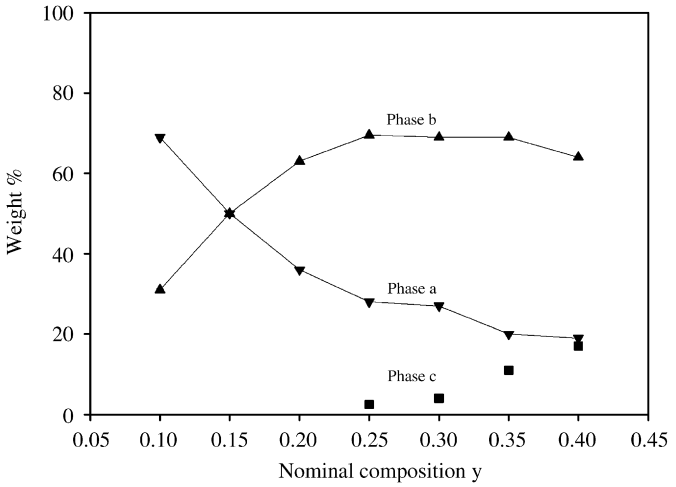

Fig. 5. Contribution of different phases according to Rietveld refinement. Two and three phase refinements were done for samples $Na_{0.8}Nb_yW_{1-y}O_3$ with nominal composition $y = 0.10$–0.20 and 0.25–0.40, respectively (symbols as given in Fig. 4).

of "phase *c*" strongly increases. With the help of microprobe analysis, it is shown (see below) that "phase *a*" corresponds to pure sodium tungsten bronze, Na_xWO_3, which appear as red-orange coloured crystals in Fig. 1. The white crystals corresponds to a composition $Na_{0.5}NbO_{2.75}$, which is related with the y independent cell parameter of about 389.7 pm. Consequently, the values of increasing lattice parameters are related to bluish coloured crystals in Fig. 1. The systematic increase in lattice parameters of "phase *b*" is related to an increasing substitution of Nb for W as reported by results of Miyamoto et al. [12], which are given for comparison in Fig. 4. These authors observed an increase in lattice parameter values for $NaW_{1-y}Nb_yO_3$ for increasing y which could tentatively be described as

$$a(y) \text{ in pm} = 4y + 386.66. \quad (4)$$

The slope here is about half of that reported by Dubson et al. [13] for the system $Na_xW_{1-y}Ta_yO_3$

$$a(x, y) \text{ in pm} = 8.21x + (0.87 + 8.07x)y + 378.45. \quad (5)$$

Eq. (5) becomes the Brown and Banks relation (Eq. (3)) for $y = 0$ which applies for the cubic Na_xWO_3 system. A similar dependency as for the system $Na_xW_{1-y}Ta_yO_3$ may also be suggested for the $Na_xW_{1-y}Nb_yO_3$ system. The results of the two-phase refinements could imply a successful substitution with x about 0.8 and an increase in y (*nominal composition*) *according to*

$$a(x, y) \text{ in pm} = 8.21x + 4y + 378.4 \quad \text{for } x \text{ close to } 1. \quad (6)$$

Microprobe analysis of "red-orange crystals" shows the presence of sodium and tungsten (Table 1). The data shows that Na/W ratios decrease with increasing y (Table 1). The cell parameter decreases from 385.01 to 384.48 pm. Using the Brown and Bank relation (Eq. (3)) [16], the composition of Na in Na_xWO_3 was calculated and show very good

Table 1
Comparison of X-ray diffraction results and EMPA results of "red-orange crystals" from the batches of nominal composition $Na_{0.8}Nb_yW_{1-y}O_3$

Nominal composition, y	Lattice parameter (pm)	Calculated Na content (Na/W) from Eq. (3)	Na/W ratio from EMPA
0.0	385.01 (2)	0.80	0.80
0.10	384.97 (1)	0.79	0.77
0.20	384.88 (2)	0.78	0.75
0.25	384.60 (2)	0.75	0.74
0.30	384.62 (2)	0.75	0.74
0.35	384.63 (2)	0.75	0.72
0.40	384.48 (10)	0.74	0.72

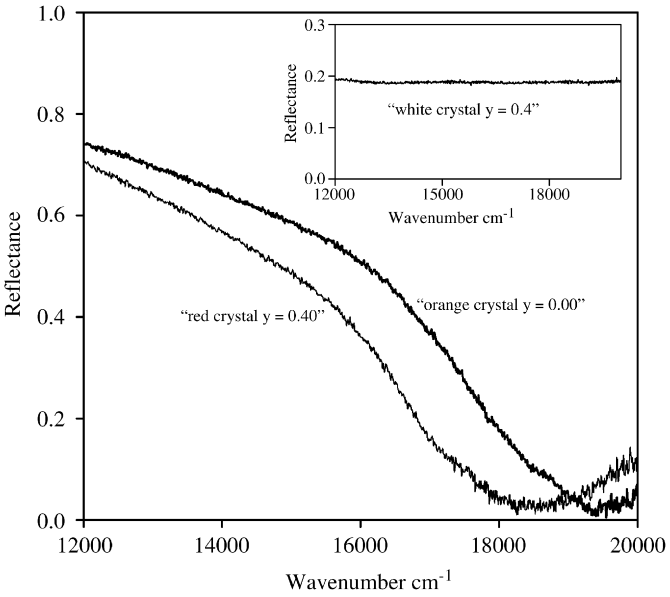

Fig. 6. Optical microreflectivity spectra of polished crystals which show Drude-type reflectivity for "red-orange" crystals with a systematic change in plasma frequency with nominal composition $Na_{0.8}Nb_yW_{1-y}O_3$ ($y = 0.40$ and 0.0) which corresponds to the composition $Na_{0.72}WO_3$ and $Na_{0.8}WO_3$, respectively (details given in text). The reflectivity of "white" crystals (inset) shows a complete flat behaviour of about 19%.

agreement to the Na/W ratio obtained from microprobe analysis (Table 1). The same effect of systematic decreasing Na content with increasing nominal y content is also obtained analysing the optical properties of the red-orange crystals by microreflection spectroscopy (Fig. 6). The spectra closely agree with spectra calculated from single crystal data given for the compositions $Na_{0.805}WO_3$ and $Na_{0.695}WO_3$ by Owen et al. [17]. These results thus independently support the systematic decrease in x of red-orange crystals with increasing nominal y as obtained by the decreasing lattice parameter (Fig. 4) and microprobe results. The optical reflectivity of the white crystals reveals a complete flat behaviour (Fig. 7) down to 1000 cm^{-1} (compare inset in Fig. 6). Below 1000 cm^{-1}, the strong increase in reflectivity can be attributed to phonon

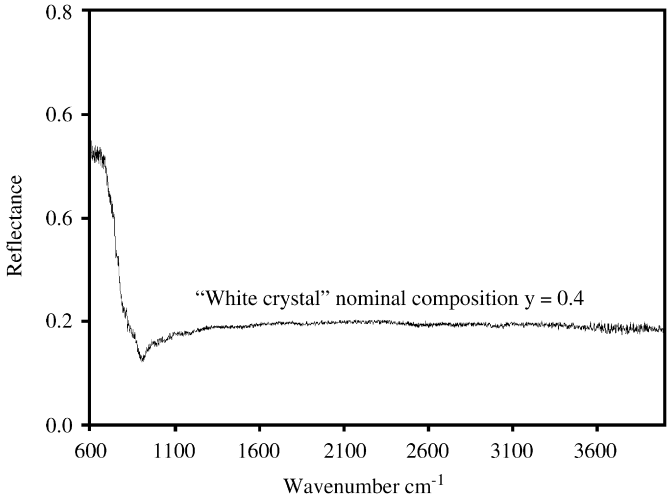

Fig. 7. The reflectivity spectrum of white crystal shows the typical appearance of strong phonon effect below 1000 cm^{-1}.

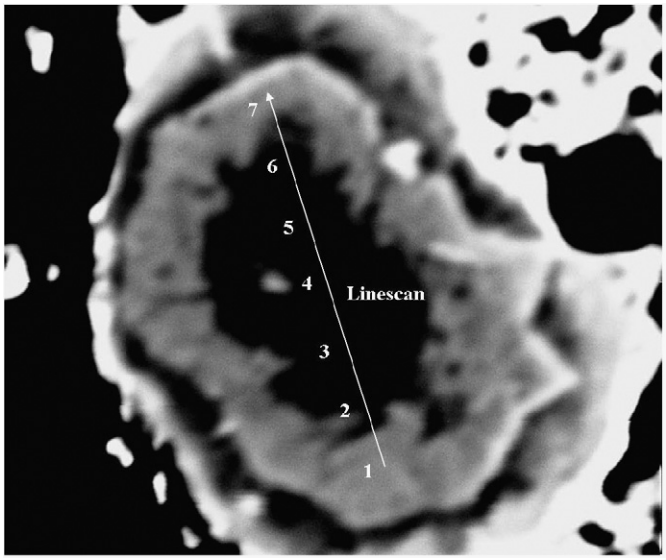

Fig. 8. Backscattered electron picture of a "white" crystal. The white arrow (of length 14 μm) corresponds to the position of the microprobe line scan. The numbers are the analysed points of performed line scan (see Table 2).

absorption, which could however not further be resolved because of the limited frequency range of the instrument.

Electron beam backscattering pictures of white crystals reveal in most cases a zoned nature concerning their chemical composition (Fig. 8). By scanning along lines as depicted in Fig. 8 obtains that the brighter parts (high scatter) contains Na, W and Nb (Table 2). In the darker inner part, the W content is below detection limit (<0.5 wt%) and only Na and Nb signals are observed.

Further data collected on the central part of the white crystals for samples having nominal composition $y = 0.25$, 0.30, 0.35 and 0.40 are given in Table 3. These data are average values from three measurement spots each

Table 2
Results of electron beam line scan of a white crystal, which is shown in Fig. 8

Points	Na (wt%)	Nb (wt%)	W (wt%)	[a]O (wt%)	Total (wt%)
1	10.13	37.05	25.26	26.07	98.51
2	8.30	55.28	5.79	28.20	97.56
3	8.26	61.34	0.71	29.47	99.78
4	7.40	61.51	0.92	29.30	99.13
5	8.33	61.21	0.52	29.39	99.45
6	10.44	37.80	26.05	26.71	101.00
7	9.61	31.65	32.55	25.47	99.28

[a]O determined by stoichiometry.

Table 3
Results of electron microprobe analysis for white crystals from batches of nominal composition $Na_{0.8}Nb_yW_{1-y}O_3$

Nominal composition, y	Average Na (wt%)	Average Nb (wt%)	Average [a]O (wt%)	Total (wt%)	Corresponding stoichiometry
0.25	7.40	63.71	30.00	101.11	$Na_{0.47}NbO_{2.73}$
0.30	7.99	61.35	29.39	99.45	$Na_{0.52}NbO_{2.78}$
0.35	7.53	62.28	29.58	99.95	$Na_{0.49}NbO_{2.76}$
0.40	7.62	61.80	29.42	99.39	$Na_{0.50}NbO_{2.76}$

[a]O determined by stoichiometry.

and only those contributions were taken where the tungsten contents were below the detection limit. The absolute values were calibrated against very pure albite ($NaAlSi_3O_8$), niobium(V)oxide (Nb_2O_5) and niobium(IV)-oxide (NbO_2) as reference. The values given in Table 3 for Na and Nb are measured absolute values in wt% elemental concentrations. The oxygen content has been calculated assuming Nb as +5 and alternatively for Nb^{4+}. With Nb taken as +5 lead to a total wt% in the range between 99.4 and 100.2 whereas for Nb^{4+} the values would become between 94.0 and 93.0 ± 0.2 wt%. The values close to 100% are very significant and indicate that Nb can be taken as +5. As an independent check we investigated the crystals of NbO_2 and Nb_2O_5 phases from samples characterized earlier [18]. The measured data (all in wt%) for the Nb content are 74.6 and 70.11 for NbO_2 and Nb_2O_5 crystals, respectively. With an adequate oxidation state for NbO_2 and Nb_2O_5 the total wt% comes out at 100.2 which show the very good reproduction for the measurement of these oxidation states by microprobe. According to this the corresponding composition of the "white crystals" (central part) can be written as $Na_{0.5\pm0.05}NbO_{2.75}$.

Raman spectroscopy study of white crystals (Fig. 9) shows peaks, which are in the same range also observed for the room temperature phase of lushite, $NaNbO_3$ [19]. The much broader peaks for $Na_{0.5}NbO_{2.75}$ may be related to the high number of vacancies and their random distribution conserving the higher symmetry. It may be noted that in all the Rietveld refinements the cubic perovskite

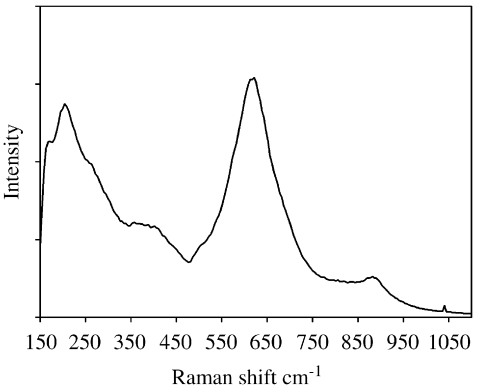

Fig. 9. Raman spectrum of white crystal.

structure with space group $Pm\bar{3}m$ *has* been used since the XRD pattern did not give any hint of a different structure type or a significant lowering of the symmetry. Thus for $Na_{0.5}NbO_{2.75}$ calculation were carried out with Nb ($\frac{111}{222}$), O ($\frac{11}{22}0$) and Na (000) with occupation factors 1, 2.75/3 and $\frac{1}{2}$, respectively. The lattice parameter obtained in the refinement reads 389.7 pm. Darlington and Knight [20] reported for cubic lushite lattice parameter values for temperatures between 920 and 1030 K, which show a linear increase with temperature according to

$$a_c(T) \text{ in pm} = 0.008T + 386.9. \quad (7)$$

Using Eq. (7), the lattice parameter of a hypothetical room temperature form of cubic lushite is estimated to be 389.2 pm. The value obtained in this investigation for the cubic perovskite $Na_{0.5}NbO_{2.75}$ is very close to the extrapolated value for the hypothetical room temperature form of a defect free cubic lushite.

The elemental composition of the bluish crystals obtained by microprobe analysis vary from crystal to crystal and imply always too large Na and Nb contents as expected from the variation in lattice parameter values (Eq. (6)). This variation may be due to varying intergrowth of bluish and white crystals.

4. Conclusion

Solid-state synthesis in the system $Na_{0.8}Nb_yW_{1-y}O_3$ with $0.0 \leqslant y \leqslant 0.4$ at 600 °C in evacuated silica tubes enables the separation of three phases. With the present synthesis conditions a slight substitution of niobium ($y \leqslant 0.07$) could be obtained as single phase. Na_xWO_3 was found to be a common phase for nominal $0.10 \leqslant y \leqslant 0.4$ and show a gradual decrease of x with increasing *nominal niobium content* along with a new perovskite-type phase of composition $Na_{0.5}NbO_{2.75}$. The new phase, $Na_{0.5}NbO_{2.75}$ could not, however, be prepared as a single phase.

Acknowledgment

The authors would like to thank Mr. Otto Diedrich for polishing the samples. Tapas Debnath is grateful to "Land Niedersachsen" for the funding "Lichtenberg Stipendium". This work has been partially financed by the Alexander von Humboldt Stiftung under collaborative research programme (V-FOKOOP/DEU/1062067/Hussain).

References

[1] Ph. Labbe, Key Eng. Mater. 68 (1991) 293.
[2] I.C. Lekshmi, A. Gayen, V. Prasad, S.V. Subramanyam, M.S. Hegde, Mater. Res. Bull. 37 (11) (2002) 1815.
[3] C.G. Granqvist, Hand Book of Inorganic Electrochromic Materials, Elsevier, Amsterdam, 1995.
[4] C.G. Granqvist, Sol. Energy Mater. Sol. Cells 60 (2000) 201.
[5] B. Ingham, S.C. Hendy, S.V. Chong, J.L. Tallon, Phys. Rev. B 72 (2005) 7.
[6] S. Raj, D. Hashimoto, H. Matsui, S. Souma, T. Sato, T. Takahashi, S. Ray, A. Chakraborty, D.D. Sarma, P. Mahadevan, W.H. McCarroll, M. Greenblatt, Phys. Rev. B 72 (2005) 125.
[7] Ch.J. Raub, A.R. Sweedler, M.A. Jensen, S. Broadston, B.T. Matthias, Phys. Rev. Lett. 13 (25) (1964) 746.
[8] A. García-Ruíz, Bokhimi, Physica C 204 (1–2) (1992) 79.
[9] A. Shengelaya, S. Reich, Y. Tsabba, K.A. Müller, Eur. Phys. J. B 12 (1999) 13.
[10] R. Brusetti, P. Haen, J. Marcus, Phys. Rev. B 65 (2002), 144528-1.
[11] P.F. Weller, B.E. Taylor, J. Solid State Chem. 2 (1970) 9.
[12] Y. Miyamoto, J.-P. Doumerc, P. Hagenmuller, S. Kume, Mater. Res. Bull. 18 (1983) 1463.
[13] M.A. Dubson, D.F. Holcomb, Phys. Rev. B 32 (4) (1985) 1955.
[14] K.E. Johansson, T. Palm, P.-E. Werner, J. Phys. E: Sci. Instrum. 13 (1980).
[15] P.-E. Werner, Ark. Kemi 31 (1969) 513.
[16] B.W. Brown, E. Banks, J. Am. Chem. Soc. 76 (1954) 963.
[17] J.F. Owen, K.J. Teegarden, H.R. Shanks, Phys. Rev. B 18 (8) (1978) 3827.
[18] C.H. Rüscher, Physica C 200 (1992) 129.
[19] Z.X. Shen, X.B. Wang, M.H. Kuok, S.H. Tang, J. Raman Spectrosc. 29 (1998) 379.
[20] C.N.W. Darlington, K.S. Knight, Acta Crystallogr. B 55 (1999) 24.